# Development of Magnetic-Silica Particles and In-house Buffers Kit for SARS-CoV-2 and CDV RNA Extraction

**Ahadi Damar Prasetya[1*], Muflikhah Muflikhah[1], Wildan Zakiah Lubis[1], Andon Insani[1], Grace Tjungirai Sulungbudi[1], Mujamilah Mujamilah[1], and Uus Saepulloh[2]**

[1]*Research Center for Radiation Detection and Nuclear Analysis Technology, Research Organization for Nuclear Energy, National Research and Innovation Agency, South Tangerang 15314, Indonesia*

[2]*Primate Research Center, Bogor Agricultural University, Bogor 16151, Indonesia*

* ***Corresponding author:***

*email: ahadi.damar.prasetya@brin.go.id*

*Received: April 10, 2023*
*Accepted: July 21, 2023*

**DOI:** 10.22146/ijc.83804

***Abstract:*** *Since the end of 2019, COVID-19 pandemic caused by the novel SARS-CoV-2 has become a serious problem for the world. Accurate and rapid techniques in testing and tracing are needed to control the virus spreading. Molecular diagnostics through gene amplification techniques, especially PCR, still become the gold standard for SARS-CoV-2 detection, which requires the first step of RNA extraction and purification. The limitations of commercial RNA extraction-purification kits during the pandemic caused a big problem in testing and tracing, especially for developing countries. A simple RNA extraction-purification kit based on magnetic-silica (MAGSi) beads and non-guanidine in-house buffers for RNA virus extraction-purification has been developed. Two types of MAGSi beads with different magnetic nanoparticles (MNPs) content were synthesized through a modified Stöber's method using the sonication technique. The PCR result shows that both the MAGSi beads and the buffer can be used as a kit for RNA extraction-purification, tested for SARS-CoV-2 and Canine Distemper Virus. Further study shows that MAGSi-1 has better RNA extraction ability, and a higher concentration of RNA has been extracted. This is likely because of the smaller particle size distribution (50–1,500 nm distribution) and higher magnetization (20.2 emu/g) of MAGSi-1 compared to MAGSi-2 with 100–1,700 nm size distribution and 14.2 emu/g magnetization.*

***Keywords:*** *buffer kit; Canine Distemper Virus; magnetic-silica; RNA extraction; SARS-CoV-2*

## ■ INTRODUCTION

Since the first case in December 2019, the coronavirus disease 2019 (COVID-19) caused by the novel severe acute respiratory syndrome coronavirus 2 (SARS-CoV-2) has been a serious problem for the world. More than 6 million people have passed away since March 2020 [1]. Many methods have been developed for SARS-CoV-2 detection in humans, such as immunological assays based on antibody or antigen detection, gene amplification techniques (polymerase chain reaction (PCR) and isothermal nucleic acid amplification), and novel developed technologies like using biosensors [2-3]. However, molecular diagnostics through gene amplification techniques, especially PCR, still become the golden standard of SARS-CoV-2 detection because it targets the pathogen's genome or proteome, making them more specific, precise, and sensitive [4-5].

In general, for RT-PCR tests, swab samples are collected from the patients, stored in viral transport media, and then sent to the laboratory for RNA extraction and purification, continued by RT-PCR [6-7]. Thus, this makes RT-PCR tests labor-intensive, and only a limited number of tests can be done daily [2,8]. Moreover, conducting RT-PCR for SARS-CoV-2 detection requires trained personnel, specialized equipment, expensive instrumentation, and a laboratory that implements biosafety level (BSL) 2 or 3 [8-10].

A way to accelerate and improve the safety of the RT-PCR testing procedure is by modifying the SARS-

CoV-2 RNA extraction and purification procedure. SARS-CoV-2 RNA extraction and purification are usually done using proteinase-k, several buffers (lysis, wash, and elution buffers), and ethanol assisted by silica spin column or magnetic-silica beads to improve the yield and purity [11-14]. RNA extraction assisted by magnetic-silica beads offers more advantages compared to silica spin columns, such as an automation option that can accelerate the extraction process and increase the number of samples and safety, easily manufactured magnetic-silica beads, and do not require specialized plasticware (spin columns, modified tips) to perform extraction [13,15].

Magnetic-silica beads are generally prepared in two steps, the synthesis of the magnetic particle core, and then the silica surface modification [16]. The magnetic particle core can be produced using several methods, including co-precipitation, microemulsion, thermal decomposition, solvothermal, sonochemical, microwave-assisted, chemical vapor deposition, combustion, carbon arc, and laser pyrolysis [17]. Then, the magnetic particle core is usually modified with a silica surface through Stöber's sol-gel method [18] because this method is relatively simple and easy to scale up compared to other methods such as microemulsion, aerosol pyrolysis, and electrochemical [16,19-23]. In Stöber's method, silica surface modification has been done through the hydrolysis and condensation reaction of tetra-ethyl-orthosilicate (TEOS) using a base catalyst, usually $NH_4OH$ [24-25]. Sonication has been also assisted by Stöber's method to obtain a uniform spherical morphology and narrow size distribution of magnetic-silica beads [23,26].

As mentioned, besides magnetic-silica beads, several solutions and liquids are used in the RNA extraction and purification process. The proteinase-k solution is used to degrade proteins [27]. The lysis buffer that usually contains detergent is used to break the cell membrane by changing the pH, solubilizing the membrane proteins, and rupturing the cell membrane to release its contents. The detergents or surfactants contained in the lysis buffers usually are sodium dodecyl sulfate (SDS), Triton X-100, Tween 20 and 80, cetyltrimethylammonium bromide (CTAB), and NP-40 [28]. In virus lysis buffer, chaotropic and hazardous salts like guanidine thiocyanate (GTC) and guanidine hydrochloride (GHCl) are also common content for inactivating the virus and denaturizing the proteins [29-31]. The wash buffer that contains a competitive agent is used for removing contaminants such as proteins and salts. Ethanol is also used in RNA extraction to precipitate nucleic acid [32]. The elution buffer usually contains high pH Tris-EDTA buffer (TE buffer) is used to elute the RNA from the silica spin column or magnetic-silica beads so that purified RNA will be released [32-33]. Further silica surface modifications and functionalization were also done to improve the binding of magnetic-silica beads and nucleic acids such as amine using aminopropyl-thiethoxysilane (APTES), thiol using (3-mercaptopropyl)trimethoxysilane (MPTMS), poly (amino ester) with multiple carboxy groups, chitosan, and epoxide [26,34-36]. However, this surface modification requires a further step, making it less efficient in time.

Extraction and purification of SARS-CoV-2 RNA assisted with silica spin column or magnetic-silica beads was based on the nucleic acid adsorption-desorption interactions on the silica surface. The interactions can be electrostatic, hydrogen bonds, van der Waals hydrophobic, or salt bridge interactions. The interaction between silanol groups on the silica surface and the nucleic acid phosphate is also regarded as a mechanism of the adsorption process [37-38]. The phosphate silanol and hydrophobic interactions are strong enough to overcome the nucleic/silica electrostatic repulsion caused by the negatively charged nucleic and silica surface, and by the addition of salt, hydrogen bonding interaction can also be increased the electrostatic repulsive force can be reduced further. Thus, nucleic acid can bind to the silica surface [31,37-38]. At low pH ($pH \leq 5$) solution, the protonated silanol groups will adsorb the nucleic acids with the presence of chaotropic salt. The elution or desorption can be done at a higher pH value without any salt since the silanol groups will be negatively charged [37].

In this research, the development of magnetic-silica beads was done using a modification of Stöber's

sol-gel method with a sonication technique. Sonochemistry has become the alternative synthesis method that has been successfully carried out in magnetic-silica synthesis [39-41]. In the sonication technique, a physical phenomenon called acoustic cavitation generates localized hot spots and produces acoustic bubbles that are considered as the storage of high potential energy, which could be released to be shock waves. These waves interact with particles and accelerate them, reaching fast collisions that enhance micro-mass transport [41]. This complex process induces acceleration of nucleation and inhibits their growth as the key factor for synthesizing nano-particles in aqueous solutions with narrow size distribution [41]. This technique has been chosen for synthesizing nanomaterial because it is simpler and more rapid than the conventional stirring method [41]. The magnetic-silica beads in this research have been prepared by sonication-assisted method with various magnetic contains to find out its effect on RNA/DNA extraction and purification application. In this study, the magnetic-silica beads' ability to assist the extraction and purification of SARS-CoV-2 RNA was also confirmed with the combination of a commercial viral nucleic extraction-purification solutions kit. A simple extraction and purification in-house buffers kit has also been developed and tested for Canine Distemper Virus (CDV) with the assistance of magnetic-silica beads. It is expected this research can be a reference to develop a simple magnetic-silica beads base, viral nucleic acid extraction, and purification kit that can be helpful to increase the testing in such a pandemic situation.

## ■ EXPERIMENTAL SECTION

### Materials

The chemicals used for the synthesis of magnetic nanoparticles ($Fe_3O_4$ NPs) and silica-coated magnetic NPs (MAGSi) are ferric chloride hexahydrate ($FeCl_3{\cdot}6H_2O$), ferrous chloride tetrahydrate ($FeCl_2{\cdot}4H_2O$), NaOH, HCl, ammonia solution 25% v/v, ethanol analytical grade, and TEOS. All chemicals were purchased from Merck and DI-water was produced using mili-Q Simplicity water purification.

The chemicals used for SARS-CoV-2 RNA extraction were confirmed positive SARS-CoV-2 samples from swab nasopharynx/oropharynx (Sample ID 6553 and 6554 from Primate Research Center, IPB University), ethanol 80%, nuclease free-water, and MagMAX™ Viral/Pathogen Nucleic Acid Isolation Kit (ThermoFisher Scientific) and synthesized magnetic-silica particles. While for the RT-PCR were Sensifast Probe No-Rox One Step Kit (Bioline-76001), 2019-nCOV RUO Kit (IDT, a mixture of 3 pairs of primer with probe of N1 and N2 specific for SARS-CoV-2 identification and RNase P marker to determine the success of RNA extraction from the samples), 2019-nCOV N Positive Control, and Hs RPP30 Positive Control.

For the CDV, RNA extractions are proteinase-K (Vivantis), in-house lysis buffer made from NaCl, Tris-Cl, and Triton X-100 from Merck, in-house elution buffer from 1× TE-buffer pH 7 (Merck), and wash buffer (ThermoFisher Scientific) and synthesized magnetic-silica particles. The reverse-transcript mRNA to cDNA using Reverse Transcriptase cDNA Synthesis kit (Inventpro). The amplification of cDNA using GoTaq Green Master Mix (Promega), 1$^{st}$ round primer (CDV 675 -F: ATTTGGGATTGCTTAGGA, CDV 1223 -R: GGCGCTCATCTTGGACAT), 2nd round primer (CDV 768 -F: GTTAGCTAGTTTCATCCT, CDV 1186 -R: GGTCCTCTGTTGTCTTGG). The gel electrophoresis used 1.8% agarose gel and 1× TAE buffer (ThermoFisher Scientific).

### Instrumentation

The crystallite phase of the MNP and MAGSi series was characterized using a X-ray diffractometer (XRD, PANalytical) with Cu Kα. The crystallite size of MNP was calculated from the X-ray diffractogram using Match! Software (Crystal Impact) at the two most intense and symmetrical peaks after profile fitting all the peaks. Fourier transform infrared (FTIR, Bruker Tensor 27) was used to analyze the functional group. A vibrating sample magnetometer (VSM, OXFORD 1.2 H) was applied to measure the magnetic saturation. Microscopy techniques using scanning electron microscopy (SEM, JEOL 2300) and transmission electron microscopy

(TEM, JEOL-JEM 1400) were used to examine the morphology of the samples. Particle size distribution measurement was done through a dynamic light scattering technique using Malvern Zetasizer NanoZS.

## Procedure

### *Synthesis of magnetic nanoparticles*

The magnetic nanoparticles have been synthesized according to Oberacker et al. [42] by the co-precipitation method. Iron chloride salts (Fe(II) and Fe(III)) with a molar ratio of 1:2, were dissolved in 60 mL of 0.1 M HCl solution. In a round bottom flask, 100 mL NaOH 2 M was added, then degassed using $N_2$ gas and heated until 80 °C. The illustration set-up of this synthesis process can be seen in Fig. 1. The solution was added dropwise using the dripping funnel into NaOH solution under vigorous stirring (>400 rpm) for 20 min until a black precipitate was formed. After the complete addition, 10 mL of ammonia 25% was introduced to the reaction mixture and stirred for a further 30 min, then cooled to room temperature. The black precipitate was magnetically separated and washed using DI-water until it reached pH 7. The product was then resuspended in 50 mL DI-water and stored in a closed container before being used.

### *Synthesis of magnetic nanoparticles-silica beads*

The magnetic nanoparticles-silica beads were synthesized based on our previous method with two different amounts of MNP (0.3 and 0.5 g) through the hydrolysis of TEOS on the surface of magnetic nanoparticles-silica beads [43]. This method synthesized magnetic nanoparticles-silica beads assisted with a cleaner-type bath (Branson 1510 with 40 kHz, 100 W).

### *SARS-CoV-2 RNA extraction and RT-PCR test*

The MAGSi were prepared in a concentration of 50 mg/mL. RNA extraction process was done using MagMAX™ Viral/Pathogen Nucleic Acid Isolation Kit protocol [44]. A mixture of MAGSi was prepared by mixing 530 µL lysis buffer with 20 µL MAGSi.

Nasopharynx/oropharynx sample digestion was done by adding 200–400 µL of the samples to 10 µL of proteinase-K, continued by adding 550 µL of the MAGSi mixture. Then, the samples were shaken for 2 min at 1050 rpm. The samples were incubated for 5 min at 65 °C, continued by MAGSi beads separation from the supernatant using an external magnet for 10 min. Next, the beads were washed by adding 1 mL of wash buffer and shaking it for 1 min at 1,050 rpm. Then, the beads were separated from the supernatant by using an external magnet for 2 min. The washing procedure was repeated two times using 1.0 and 0.5 mL of ethanol 80%. After washing, the MAGSi beads were dried by shaking at 1050 rpm for 2 min. The elution of RNA was done by adding 50–100 µL elution buffer to the MAGSi beads, continued by shaking at 1050 rpm for 5 min. The beads were incubated at 65 °C for 10 min, continued by shaking at 1050 rpm. The MAGSi beads were separated using an external magnet for 3 min. The eluted RNA on the supernatant was analyzed further by spectrometry technique using Nanodrop OneC Spectrophotometer (Thermo Scientific) at 260 and 280 nm and RT-PCR.

Prior to the RT-PCR process, two kinds of master mix were prepared. The master mix was composed of 1.8 µL Primer mix (N1 for the master mix I and N2 for master mix 2), 0.2 µL Reverse Transcriptase, 0.4 µL Ribosafe RNAse Inhibitor, 10 µL Sensifast one-step kit mix and 8 µL of RNA from the extraction process. The RT-PCR was done using Quanstudio5 thermocycler (Applied Biosystem) with the program as in Table 1.

### *CDV RNA extraction and PCR test*

The MAGSi were prepared in a concentration of 50 mg/mL. RNA extraction process has been carried out using MagMAX™ Viral/Pathogen Nucleic Acid Isolation

**Table 1.** RT-PCR program

| Temperature (°C) | Time | Cycles | Notes |
|---|---|---|---|
| 45 | 10 min | 1 | Reverse transcription |
| 95 | 2 min | 1 | Polymerase activation |
| 95 | 5 s | 40 | Denaturation |
| 55 | 20 s | | Annealing/extension (acquire at the end of step) |
| 4 | ∞ | | |

Kit protocol [44]. A mixture of MAGSi was prepared by mixing 530 µL in-house lysis buffer with 20 µL MAGSi.

The CDV samples were digested by adding 200–400 µL of the samples to 10 µL of proteinase-K, continued by the addition of 550 µL of the MAGSi mixture. Then, the samples were shaken for 2 min at 1,050 rpm. The samples were incubated for 5 min at 65 °C, continued by MAGSi beads separation from the supernatant using an external magnet for 10 min. Next, the beads were washed using 1 mL of wash buffer and then shaked for 1 min at 1050 rpm. The beads were separated from the supernatant using an external magnet for 2 min. The washing procedure was repeated two times using 1.0 and 0.5 mL of ethanol 80%. After the washing process, the MAGSi beads were dried by shaking at 1,050 rpm for 2 min. The elution of RNA was done by adding 50–100 µL in-house elution buffer to the MAGSi beads, followed by shaking at 1050 rpm for 5 min. The beads were incubated at 65 °C for 10 min, continued by shaking at 1,050 rpm for mins. The MAGSi beads were separated using an external magnet for 3 min. The eluted RNA on the supernatant was analyzed further by spectrometry technique using Nanodrop OneC Spectrophotometer (Thermo Scientific) at 260 and 280 nm and RT-PCR.

Reverse Transcript mRNA to cDNA was done using Reverse Transcriptase cDNA Synthesis kit (Inventpro). The extracted sample mRNA was added into 12 µL master mix (1 µL random hexamer/oligo dT, 1 µL dNTPs, 2 µL 10 RT buffer, 4 µL $MgCl_2$, 2 µL 0.1 DTT, 1 µL RT Inventpro enzyme, 1 µL nuclease-free water). The reverse transcript reaction was done using Veriti Thermal Cycler (Thermo Fisher Scientific) with the condition of 50 °C for 30 min, continued by 4 °C for 2 min.

Amplification of cDNA was done by polymerase chain reaction. The PCR reagent was made from 1 µL F Primer 10 pmol/µL, 1 µL R Primer pmol/µL, 12.5 µL GoTaq Green Master Mix, up to 25 µL nuclease-free water, and 2.5–5.0 µL cDNA sample. The PCR reaction was done in Veriti Thermal Cycler (Thermo Fisher Scientific) with the condition as in Table 2.

Then the electrophoresis procedure of PCR product was performed using 1.8% agarose gel for 45 min in 1× TAE buffer at 100 V. GelDoc with Quantity one software was used to visualize the gel.

## ■ RESULTS AND DISCUSSION

### Characterization of MNPs, MAGSi-1 and MAGSi-2

The success of silica coatings at the MNPs surface can be seen from the FTIR spectra in Fig. 1 and the XRD in Fig. 2. All curves show bands at around 570 $cm^{-1}$ corresponding to the Fe–O stretching vibration related to the magnetite [45-47]. The bands at 1,070 and 798 $cm^{-1}$ from the MAGSi-1 and MAGSi-2 spectra correspond to the Si–O–Si asymmetric and symmetric stretching vibration, while the band around 960 $cm^{-1}$ was from the Si–O stretching vibration. The bands

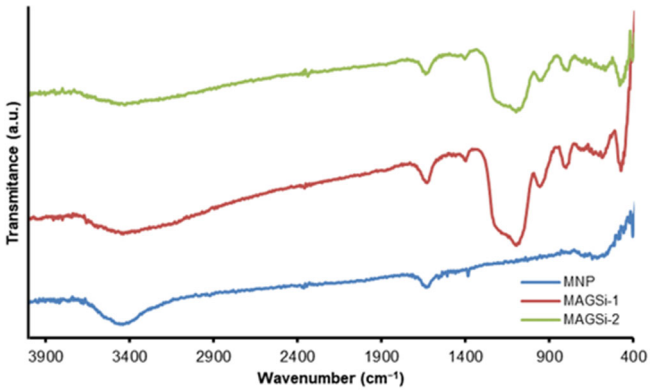


**Fig 1.** FTIR spectra of MAG, MAGSi-1, and MAGSi-2

**Table 2.** PCR program

| Temperature (°C) | Time (s) | Cycles | Notes |
|---|---|---|---|
| 94 | 180 | 1 | Denaturation |
| 94 | 30 | | Denaturation |
| 54 | 30 | 40 | Annealing |
| 72 | 60 | | Extension |
| 72 | 300 | 1 | Extension |
| 4 | ∞ | 1 | Refrigeration |

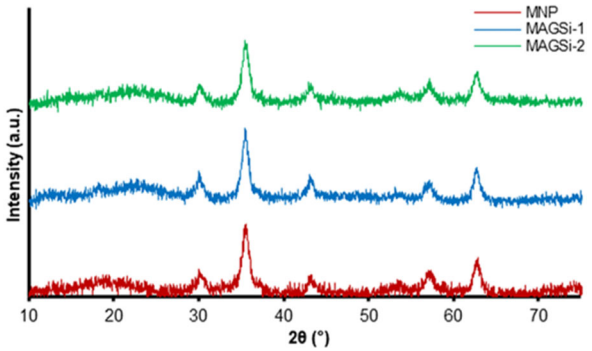


**Fig 2.** XRD of MNP, MAGSi-1, and MAGSi-2

around 1,625 and 3,425 $cm^{-1}$ can be assigned to the O–H stretching and bending from the Si–OH or adsorbed water molecules at the surface of the samples.

The XRD in Fig. 2 from the MAG-Si samples and MNP show peaks at 2θ of 30.4°, 35.7°, 43.2°, 57.1°, and 62.5° correspond to the (220), (311), (400), (422), and (511) crystal planes from $Fe_3O_4$ respectively. Furthermore, an additional broad peak can be seen at the MAG-Si samples diffractograms at 23° that belongs to amorphous silica, which confirms that magnetic-silica composites have been formed.

The DLS measurements in Fig. 3 show that MNPs have a particle size distribution ranging from 30 to 600 nm with a polydispersity index (PdI) of 0.381, while the TEM image in Fig. 4(a-c) shows smaller MNPs single particle with size more than 10 nm. The average crystallite size of MNPs calculated from the XRD was 10.5 nm, which is consistent with the particle size calculated from the TEM images in Fig. 4(a-c).

The larger size was obtained on the DLS technique because the technique measures the hydrodynamic size of the particles and the tendency of MNPs to agglomerate. The agglomeration tendency of MNPs can be seen in Fig. (4a-c), and the DLS measurement result in Fig. 3(b) shows that after several measurements, the size distribution graph shifts to a larger particle size. It is also interesting to notice that based on a quick glance at the TEM images, MAGSi-2 has more MNPs in the core compared to MAGSi-1 due to more MNPs being used for MAGSi-2.

Meanwhile, MAGSi-1 distribution size ranges from 50–1,500 nm with a PdI of 0.430 and MAGSi-2 from 100–1,700 nm with a PdI of 0.249. Both MAGSi samples

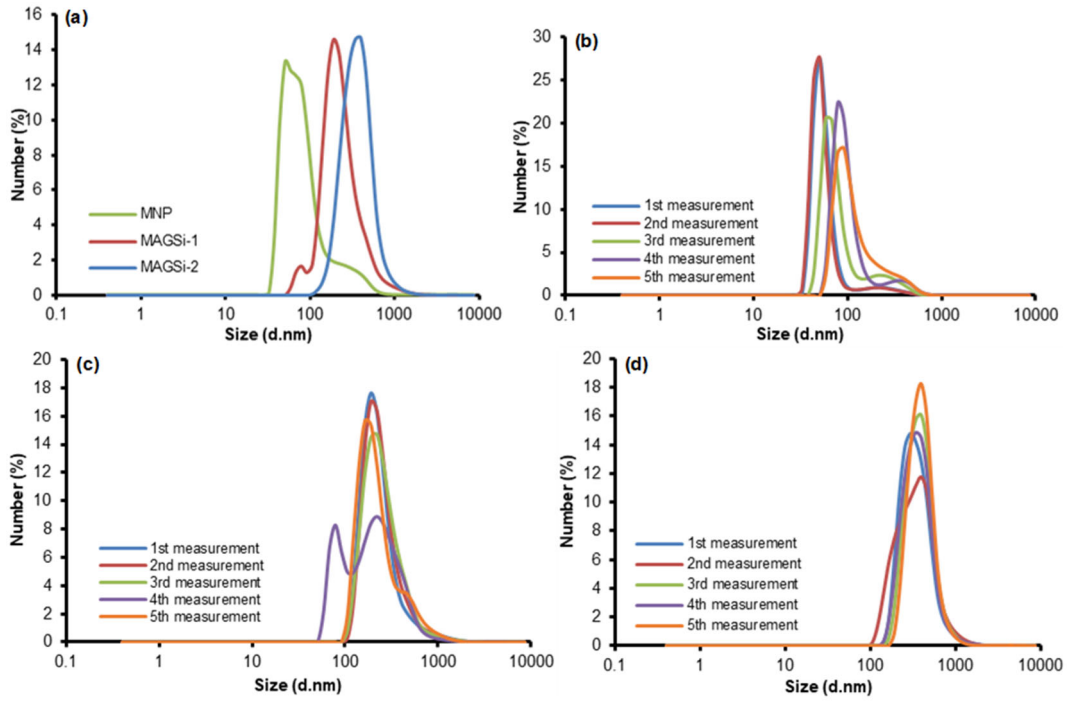


**Fig 3.** Comparison of MNP, MAGSi-1, MAGSi-2 size distribution by (a) average measurement, (b) size distribution measurement 1 to 5 of MNP, (c) MAGSi-1, (d) MAGSi-2

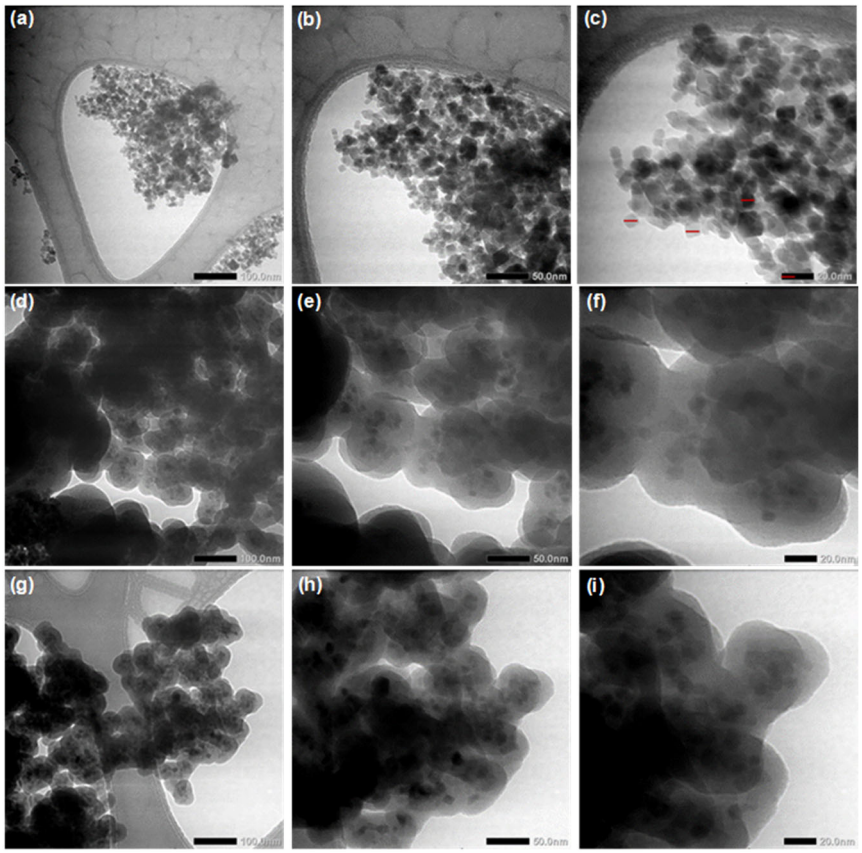


**Fig 4.** TEM images of (a-c) MNP, (d-f) MAGSi-1, and (g-i) MAGSi-2

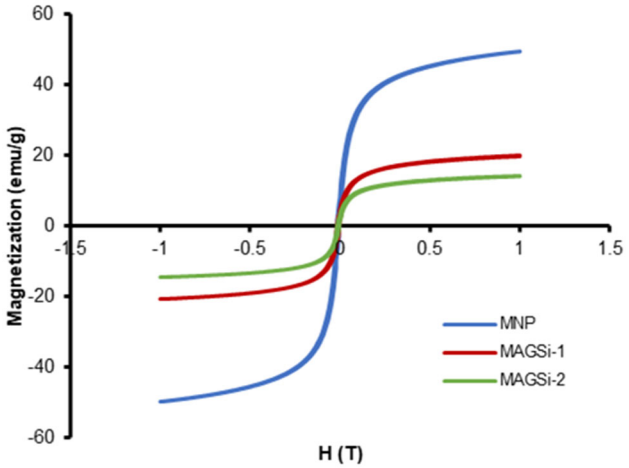


**Fig 5.** Magnetization curves of MNP (blue), MAGSi-1 (red) and MAGSi-2 (green)

have a raisin-bun morphology with several discrete cores of MNPs inside the silica matrix [48]. No agglomeration tendency was found as the DLS measurement shows no change after several measurements, as in Fig. 3(c-d). However, MAGSi particles tend to form aggregated particles due to the siloxane bridge that formed between the raisin-bun structure during the TEOS polymerization reaction [49].

Fig. 5 shows the magnetic saturation of MAG, MAGSi-1, and MAGSi-2 with the value of 49.5, 20.2, and 14.2 emu/g, respectively. The magnetization curves of all samples do not show any hysteresis loop, indicating that MNPs are superparamagnetic [50]. The silica layer of the MAGSi samples decreases the magnetic saturation. MAGSi-1 has a higher magnetic saturation than MAGSi-2 because of the higher MNPs composition.

## SARS-CoV-2 RNA Extraction by MAGSi Samples and Confirmation Using RT-PCR

Table 3 shows extracted RNA concentration of MAGSi samples while Table 4 shows the RT-PCR result of the extracted RNA using MAGSi samples. The concentration data shows that MAGSi-1 has better RNA extraction ability compared to MAGSi-2, with higher RNA extracted concentration. This phenomenon can

**Table 3.** SARS-CoV-2 RNA concentration was extracted using different types of magnetic beads

| Sample ID | SARS-CoV-2 RNA concentration (ng/μL) | |
|---|---|---|
| | MAGSi-1 | MAGSi-2 |
| 6553 | 28.4 | 13.2 |
| 6554 | 44.4 | 12.7 |

happen because MAGSi-1 has a smaller particle size than MAGSi-2, resulting in a higher surface area and more silanol groups on the surface for RNA adsorption [51].

The RT-PCR data in Table 4 also confirms that SARS-CoV-2 RNA was successfully extracted, and the genes were successfully amplified. However, the Ct values of the RT-PCR data cannot be used directly for estimating the viral load or judging which MAGSi samples is better regarding the extraction and purification ability because of many factors from the sampling until the RNA amplification process [52].

## Canine Distemper Virus (CDV) RNA Extraction by MAGSi and Confirmation Using PCR

Further RNA extraction tests using MAGSi samples were done using CDV and our in-house lysis and elution buffer. The CDV was chosen since it has several similar characteristics to SARS-CoV-2. Both viruses are enveloped RNA viruses, with SARS-CoV-2 as a (−) RNA virus and CDV as a (+) RNA virus. Furthermore, CDV is non-infectious for humans, making it safe for experiments.

The extracted CDV RNA concentration data obtained from the spectroscopy technique is presented in Table 5. The result again indicates that MAGSi-1 extracted 10.2 ng/μL RNA, which is higher compared to MAGSi-2 (8.7 ng/μL). The MAGSi samples also have a higher RNA extracted concentration than commercial nucleic extraction magnetic beads (MAGMAX) due to the higher concentration of MAGSi beads that have been used. This indicates, in the same concentration of magnetic beads, MAGSi beads have a comparable result with the commercial magnetic beads. The RNA concentration data also can be obtained even though the extraction-purification process was done using the in-house buffer. This shows that the in-house buffers were able to lysis the viruses and elute the RNA.

**Table 4.** RT-PCR results of extracted SARS-CoV-2 RNA

| Type of magnetic beads | Sample ID[1)] | Target Gen[2)] | | |
|---|---|---|---|---|
| | | N1 SARS COV-2 | N2 SARS COV-2 | Human RNase P |
| MAGSi-1 | 6553 | 28.04 | 29.85 | 24.36 |
| | 6554 | 35.48 | 38.09 | 32.51 |
| MAGSi-2 | 6553 | 27.33 | 27.89 | 24.76 |
| | 6554 | 33.76 | 33.64 | 27.76 |
| Commercial kit | 6553 | 27.55 | 26.78 | 24.89 |
| | 6554 | 32.34 | 33.76 | 27.68 |
| | NTC (negative control) | N. A | N. A | N. A |
| | Positive control | 27.36 | 26.55 | 28.65 |

[1)]The sample used is a nasopharyngeal/oropharyngeal swab sample that has been confirmed positive for SRAS Cov-2

[2)]The genes that used as target for detected are: N1 and N2 originating from the SARS Cov-2 virus, and the human gene RNaseP as a control to confirm the success of the extraction process

**Table 5.** CDV RNA concentration extracted using different types of magnetic beads with in house type of buffer

| Type of magnetic beads | Magnetic beads concentration (mg/mL) | CDV RNA concentration (ng/μL) |
|---|---|---|
| MAGSi-1 | 50 | 10.2 |
| MAGSi-2 | 50 | 8.7 |
| MAGMAX (Commercial kit) | 30 | 5.3 |

Gel-electrophoresis procedure was done to confirm that the virus RNA was successfully extracted, reverse-transcripted, and amplified. The bright bands on 450 bp for the MAGSi-1, MAGSi-2, and MAGMAX in-house buffers indicate that the three processes mentioned have been successfully carried out (Fig. 6).

A simple cost analysis of this developing kit is presented in Table 6, and the comparison with other available commercial brands can be seen in Table 7. Based on calculation, for one batch of MAG and MAG-Si, the price of chemicals needed were 46,728 IDR and 208,932 IDR respectively, which is much cheaper than other brands. This price can be a good reference for developed countries to make their own magnetic-silica product, especially for DNA or RNA extraction since, in a pandemic situation extraction kits can be hard to find in the market. However, a detailed analysis of the pricing is

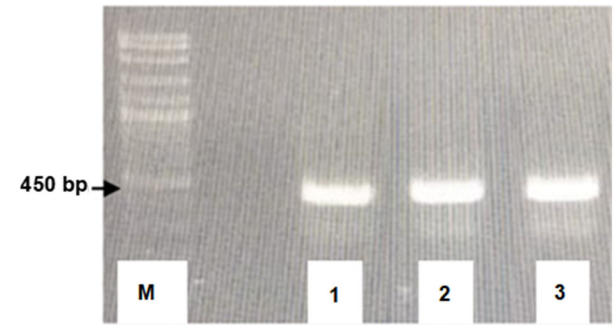


**Fig 6.** Gel electrophoresis images of amplified CDV RNA extracted using (1) MAGSi-1 and in-house buffers, (2) MAGSi-2 and in-house buffers, MAGMAX and in-house buffers (3)

**Table 6.** Simple cost analysis of our MAG-Si products

| Chemicals | Price (USD)* | Price (IDR)** | Price per g or mL (IDR) | Price (IDR)*** |
|---|---|---|---|---|
| $FeCl_3 \cdot 6H_2O$, for analysis EMSURE® ACS, Reag. Ph Eur (250 g) | 113.00 | 1,808,000 | 7,232 | 23,432 |
| $FeCl_2 \cdot 4H_2O$, for analysis EMSURE® (250 g) | 141.00 | 2,256,000 | 9,024 | 18,048 |
| Ammonia solution 25%, for analysis EMSURE® ISO, Reag. Ph Eur (2.5 L) | 70.70 | 1,131,200 | 525 | 5,248 |
| Total Price | 324.70 | 5,195,200 | - | 46,728 |
| Synthesis of MAG-Si | | | | |
| MAG (2 g)**** | - | 46,728 | 23,364 | 11,682 |
| TEOS for synthesis (250 mL) | 50.00 | 800,000 | 3,200 | 12,800 |
| Ammonia solution 25%, for analysis EMSURE® ISO, Reag. Ph Eur (2.5 L) | 70.70 | 1,131,200 | 525 | 5,250 |
| Ethanol absolute EMPLURA® (2.5 L) | 140.00 | 2,240,000 | 896 | 179,200 |
| Total Price | - | - | - | 208,932 |

Assumptions: *Price was based on the Sigma-Aldrich website per 9 June 2023
**Conversion rate used in this calculation was 1 USD = 16,000 IDR
***Price based on usage is based on our method (IDR)
****Assuming each synthesis of MAG can produce 2 g of MAG

**Table 7.** Comparison of MAG-Si with other available commercial brands

| Brand | Price (USD) | Price (IDR)** | Price per extraction (IDR) |
|---|---|---|---|
| MAG-Si 50 mg/mL (20 mL) (100 reactions) | - | 208,932 | 209 |
| MagMAX™ Viral/Pathogen Binding Beads, Applied Biosystems™ (20 mL) (100 reactions)* | 944.00 | 15,104,000 | 15,104 |
| MagAttract Suspension G Qiagen (13 ml) (100 reactions)* | 332.00 | 5,312,000 | 5,312 |

Assumptions: *Price was based on the brand website per 9 June 2023
**Conversion rate used in this calculation was 1 USD = 16,000 IDR

still needed since we have not included some other price components such as buffers included in the kit, product analysis, taxes, employee wages, etc.

Moreover, the sonochemical approach in this study can provide several advantages especially better size distribution (narrow) and acceleration of the TEOS hydrolysis, as mentioned in the previous study [39,53]. However, providing MAGSi and an in-house kit buffer in this research as an alternative reagent for SARS-CoV-2 testing still requires optimization and customization to meet clinical requirements.

## ■ CONCLUSION

In this work, the synthesis of two types of MAGSi has been done through the sonication technique. Both samples have a similar phase and functional group. However, MAGSi-2 has a smaller size and higher magnetization due to higher MNP contents. MAGSi-2, which has higher MNP contents, shows better extraction ability on SARS-CoV-2 and CDV samples compared to MAGSi-1 due to smaller particle size, which leads to higher surface area for RNA adsorption. Higher MNP content also increases the speed of magnetic separation, making the extraction process faster. In comparison with other available commercial brands, the MAGSi seems to have a lower production price. In-house buffers have also been developed and tested for extracting SARS-CoV-2 and CDV RNA. The buffers show a promising ability for SARS-CoV-2, and CDV RNA extraction, combined with MAGSi-2, higher RNA concentration can be achieved.

## ■ ACKNOWLEDGMENTS

The authors gratefully acknowledge the financial support of Research and Innovation Funding for Advanced Indonesia (RIIM) No. contract B-811/II.7.5/FR/6/2022 and B-2103/III.2/HK.04.037/2022, titled Nanoparticle Magnetic-Silica (MAG-Si) Development for Extraction and Purification Application of SARS-Cov-2 RNA Virus in the RT-PCR Detection Process.

## ■ AUTHOR CONTRIBUTIONS

Ahadi Damar Prasetya conducted the experiment and wrote the original draft; Muflikhah conducted the experiment and edited the draft; Wildan Zakiah Lubis conducted VSM analysis; Andon Insani concepted and reviewed draft, Grace Tjungirai Sulungbudi: conducted PSA data analysis, Mujamilah: analyzed VSM data, concepted and reviewed draft, Uus Saepuloh: conducted RNA extraction and PCR test.

## ■ REFERENCES

[1] WHO, 2020, *WHO Coronavirus (COVID-19) Dashboard with Vaccination Data*, https://data.who.int/dashboards/covid19/vaccines?n=c, accessed March 14, 2022.

[2] Yüce, M., Filiztekin, E., and Özkaya, K.G., 2021, COVID-19 diagnosis: A review of current methods, *Biosens. Bioelectron.*, 172, 112752.

[3] Khandia, R., Singhal, S., Alqahtani, T., Kamal, M.A., El-Shall, N.A., Nainu, F., Desingu, P.A., and Dhama, K., 2022, Emergence of SARS-CoV-2 Omicron (B.1.1.529) variant, salient features, high global health concerns and strategies to counter it amid ongoing COVID-19 pandemic, *Environ. Res.*, 209, 112816.

[4] Chang K.P., Lin Z.Y., Hung M.C., and Hsieh B.S., 2011, Effects of irradiation on chitosan-coated nanoparticles for hyperthermia, *Adv. Mater. Res.*, 311-313, 419–431.

[5] Namagerdi, A.A., Ciani, F., d'Angelo, D., Napolitano, F., Avallone, L., Napolitano, F., and Avallone, L., 2022, Covid-19, environment, clinicopathologic features, laboratory findings and diagnosis, treatment, vaccines, animals, and cancer, *Ann. Res. Oncol.*, 2 (1), 34–54.

[6] Cheng, M.P., Papenburg, J., Desjardins, M., Kanjilal, S., Quach, C., Libman, M., Dittrich, S., and Yansouni, C.P., 2020, Diagnostic testing for severe acute respiratory syndrome–related Coronavirus 2, *Ann. Intern. Med.*, 172 (11), 726–734.

[7] Morehouse, Z.P., Samikwa, L., Proctor, C.M., Meleke, H., Kamdolozi, M., Ryan, G.L., Chaima, D., Ho, A., Nash, R.J., and Nyirenda, T.S., 2021, Validation of a direct-to-PCR COVID-19 detection protocol utilizing mechanical homogenization: A model for reducing resources needed for accurate testing, *PLoS One*, 16 (8), e0256316.

[8] Colbert, A.J., Lee, D.H., Clayton, K.N., Wereley, S.T., Linnes, J.C., and Kinzer-Ursem, T.L., 2022, PD-LAMP smartphone detection of SARS-CoV-2 on chip, *Anal. Chim. Acta*, 1203, 339702

[9] Nyaruaba, R., Mwaliko, C., Hong, W., Amoth, P., and Wei, H., 2021, SARS-CoV-2/COVID-19 laboratory biosafety practices and current molecular diagnostic tools, *J. Biosaf. Biosecur.*, 3 (2), 131–140.

[10] Das, D., Hsieh, H.C., Chen, C.S., Chen, W.L., and Chuang, H.S., 2022, Ultrafast and sensitive screening of pathogens by functionalized Janus microbeads-enabled rotational diffusometry in combination with isothermal amplification, *Small Sci.*, 2 (5), 2200010.

[11] Shin, J.H., 2013, "Nucleic Acid Extraction Techniques" in *Advanced Techniques in Diagnostic Microbiology*, Eds. Tang, Y.W., and Stratton, C.W., Springer US, Boston, MA, 209–225.

[12] Ambrosi, C., Prezioso, C., Checconi, P., Scribano, D., Sarshar, M., Capannari, M., Tomino, C., Fini, M., Garaci, E., Palamara, A.T., De Chiara, G., and Limongi, D., 2021, SARS-CoV-2: Comparative analysis of different RNA extraction methods, *J. Virol. Methods*, 287, 114008.

[13] Klein, S., Müller, T.G., Khalid, D., Sonntag-Buck, V., Heuser, A.M., Glass, B., Meurer, M., Morales, I., Schillak, A., Freistaedter, A., Ambiel, I., Winter, S.L., Zimmermann, L., Naumoska, T., Bubeck, F., Kirrmaier, D., Ullrich, S., Barreto Miranda, I., Anders, S., Grimm, D., Schnitzler, P., Knop, M., Kräusslich, H.G., Dao Thi, V.L., Börner, K., and Chlanda, P., 2020, SARS-CoV-2 RNA extraction using magnetic beads for rapid large-scale testing by RT-qPCR and RT-LAMP, *Viruses*, 12 (8), 863.

[14] Haile, S., Nikiforuk, A.M., Pandoh, P.K., Twa, D.D.W., Smailus, D.E., Nguyen, J., Pleasance, S., Wong, A., Zhao, Y., Eisler, D., Moksa, M., Cao, Q., Wong, M., Su, E., Krzywinski, M., Nelson, J., Mungall, A.J., Tsang, F., Prentice, L.M., Jassem, A., Manges, A.R., Jones, S.J.M., Coope, R.J., Prystajecky, N., Marra, M.A., Krajden, M., and Hirst, M., 2022, Optimization of magnetic bead-based nucleic acid extraction for SARS-CoV-2 testing using readily available reagents, *J. Virol. Methods*, 299, 114339.

[15] He, H., Li, R., Chen, Y., Pan, P., Tong, W., Dong, X., Chen, Y., and Yu, D., 2017, Integrated DNA and RNA extraction using magnetic beads from viral pathogens causing acute respiratory infections, *Sci. Rep.*, 7 (1), 45199.

[16] Setyawan, H., Fajaroh, F., Widiyastuti, W., Winardi, S., Lenggoro, I.W., and Mufti, N., 2012, One-step synthesis of silica-coated magnetite nanoparticles by electrooxidation of iron in sodium silicate solution, *J. Nanopart. Res.*, 14 (4), 807.

[17] Majidi, S., Zeinali Sehrig, F., Farkhani, S.M., Soleymani Goloujeh, M., and Akbarzadeh, A., 2016, Current methods for synthesis of magnetic nanoparticles, *Artif. Cells, Nanomed., Biotechnol.*, 44 (2), 722–734.

[18] Stöber, W., Fink, A., and Bohn, E., 1968, Controlled growth of monodisperse silica spheres in the micron size range, *J. Colloid Interface Sci.*, 26 (1), 62–69.

[19] Mahajan, R., Suriyanarayanan, S., and Nicholls, I.A., 2021, Improved solvothermal synthesis of γ-$Fe_2O_3$ magnetic nanoparticles for $SiO_2$ coating, *Nanomaterials*, 11 (8), 1889.

[20] Sharafi, Z., Bakhshi, B., Javidi, J., and Adrangi, S., 2018, Synthesis of silica-coated iron oxide nanoparticles: Preventing aggregation without using additives or seed pretreatment, *Iran. J. Pharm. Res.*, 17 (1), 386–395.

[21] Asab, G., Zereffa, E.A., and Abdo Seghne, T., 2020, Synthesis of silica-coated $Fe_3O_4$ nanoparticles by microemulsion method: Characterization and evaluation of antimicrobial activity, *Int. J. Biomater.*, 2020, 4783612.

[22] Pham, X.H., Kyeong, S., Jang, J., Kim, H., Kim, J., Jung, S., Lee, Y.S., Jun, B.H., and Chung, W.J., 2016, Facile method for preparation of silica coated monodisperse superparamagnetic microspheres, *J. Nanomater.*, 2016, 1730403.

[23] Bui, T.Q., Ngo, H.T.M., and Tran, H.T., 2018, Surface-protective assistance of ultrasound in synthesis of superparamagnetic magnetite nanoparticles and in preparation of mono-core magnetite-silica nanocomposites, *J. Sci.: Adv. Mater. Devices*, 3 (3), 323–330.

[24] Harris, M.T., Brunson, R.R., and Byers, C.H., 1990, The base-catalyzed hydrolysis and condensation reactions of dilute and concentrated TEOS solutions, *J. Non-Cryst. Solids*, 121 (1), 397–403.

[25] Cihlář, J., 1993, Hydrolysis and polycondensation of ethyl silicates. 1. Effect of pH and catalyst on the hydrolysis and polycondensation of tetraethoxysilane (TEOS), *Colloids Surf., A*, 70 (3), 239–251.

[26] Mohammed, M.A.A., Chen, Z., Li, K., and Zhang, B., 2022, The study of $Fe_3O_4$@$SiO_2$-$NH_2$ nano-magnetic composite modified by glutaraldehyde to immobilized penicillin G acylase, *Turk. J. Chem.*, 46 (1), 103–115.

[27] Ndiritu, W., Cawthorn, R.J., and Kibenge, F.S.B., 1994, Use of proteinase K in the excystation of *Sarcocystis cruzi* sporocysts for *in vitro* culture and DNA extraction, *Vet. Parasitol.*, 52 (1), 57–60.

[28] Shehadul Islam, M., Aryasomayajula, A., and Selvaganapathy, P.R., 2017, A review on macroscale and microscale cell lysis methods, *Micromachines*, 8 (3), 83.

[29] Farrell, R.E., 2017, "Chapter 3 - RNA Isolation Strategies" in *RNA Methodologies (Fifth Edition)*, Academic Press, Cambridge, MA, US, 75–115.

[30] Davies, K., Arnold, U., Buczkowski, H., Burton, C., Welch, S.R., Green, N., Strachan, R., Beetar-King, T., Spencer, P., Hettiarachchi, N., Hannah, M.J., Jones, M., Cane, P.A., Bruce, C.B., Woodford, N., Roberts, A.D.G., and Killip, M.J., 2021, Virucidal efficacy of guanidine-free inactivants and rapid test buffers against SARS-CoV-2, *Sci. Rep.*, 11 (1), 23379.

[31] Sun N., Deng, C., Liu, Y., Zhao, X., Tang, Y., Liu, R., Xia, Q., Yan, W., and Ge, G., 2014, Optimization of influencing factors of nucleic acid adsorption onto silica-coated magnetic particles: Application to viral nucleic acid extraction from serum, *J. Chromatogr. A*, 1325, 31–39.

[32] Shin, J.H., 2018, "Nucleic Acid Extraction and Enrichment" in *Advanced Techniques in Diagnostic Microbiology: Volume 1: Techniques*, Eds. Tang, Y.W., and Stratton, C.W., Springer International Publishing, Cham, Germany, 273–292.

[33] Gjerde, D.T., Hoang, L., and Hornby, D., 2009, *RNA Purification and Analysis: Sample Preparation, Extraction, Chromatography*, Wiley-VCH, Weinheim, Germany.

[34] Digigow, R.G., Dechézelles, J.F., Dietsch, H., Geissbühler, I., Vanhecke, D., Geers, C., Hirt, A.M., Rothen-Rutishauser, B., and Petri-Fink, A., 2014, Preparation and characterization of functional silica hybrid magnetic nanoparticles, *J. Magn. Magn. Mater.*, 362, 72–79.

[35] Tiwari, A.P., Satvekar, R.K., Rohiwal, S.S., Karande, V.A., Raut, A.V., Patil, P.G., Shete, P.B., Ghosh, S.J., and Pawar, S.H., 2015, Magneto-separation of genomic deoxyribose nucleic acid using pH responsive $Fe_3O_4$@silica@chitosan nanoparticles in biological samples, *RSC Adv.*, 5 (11), 8463–8470.

[36] Zhang, Z.C., Yuan, C., and Wan, Q.H., 2007, Surface modification of magnetic silica microspheres and its application to the isolation of plant genomic nucleic acids, *Chin. J. Anal. Chem.*, 35 (1), 31–36.

[37] Chen, W.Y., Matulis, D., Hu, W.P., Lai, Y.F., and Wang W.H., 2020, Studies of the interactions mechanism between DNA and silica surfaces by isothermal titration calorimetry, *J. Taiwan Inst. Chem. Eng.*, 116, 62–66.

[38] Wu, J., Wang, H., Zhu, A., and Long, F., 2018, Adsorption kinetics of single-stranded DNA on functional silica surfaces and its influence factors: An evanescent-wave biosensor study, *ACS Omega*, 3 (5), 5605–5614.

[39] Morel, A.L., Nikitenko, S.I., Gionnet, K., Wattiaux, A., Lai-Kee-Him, J., Labrugere, C., Chevalier, B., Deleris, G., Petibois, C., Brisson, A., and Simonoff, M., 2008, Sonochemical approach to the synthesis of $Fe_3O_4$@$SiO_2$ core–shell nanoparticles with tunable properties, *ACS Nano*, 2 (5), 847–56.

[40] Fuentes-García, J.A., Carvalho Alavarse, A., Moreno Maldonado, A.C., Toro-Córdova, A., Ibarra, M.R., and Goya, G.F., 2020, Simple sonochemical method to optimize the heating efficiency of magnetic nanoparticles for magnetic fluid hyperthermia, *ACS Omega*, 5 (41), 26357–26364.

[41] Ali Dheyab, M., Abdul Aziz, A., and Jameel, M.S., 2021, Recent advances in inorganic nanomaterials synthesis using sonochemistry: A comprehensive

review on iron oxide, gold and iron oxide coated gold nanoparticles, *Molecules*, 26 (9), 2453.

[42] Oberacker, P., Stepper, P., Bond, D.M., Höhn, S., Focken, J., Meyer, V., Schelle, L., Sugrue, V.J., Jeunen, G.J., Moser, T., Hore, S.R., von Meyenn, F., Hipp, K., Hore, T.A., and Jurkowski, T.P., 2019, Bio-On-Magnetic-Beads (BOMB): Open platform for high-throughput nucleic acid extraction and manipulation, *PLoS Biol.*, 17 (1), e3000107.

[43] Prasetya, A.D., Muflikhah, M., Lubis, W.Z., Arif, M.F., Sulungbudi, G.T., Mujamilah, M., and Insani, A., 2023, Synthesis method variations effects on magnetic-silica particles characteristics and its potential for nucleic acid adsorption, *AIP Conf. Proc.*, 2902 (1), 080005.

[44] Anonymous, 2020, *User Guide: MagMAX™ Viral/Pathogen Nucleic Acid Isolation Kit*, Thermo Fisher Scientific Inc., Waltham, MA, US.

[45] Zhang, L., Shao, H.P., Zheng, H., Lin, T., and Guo, Z.M., 2016, Synthesis and characterization of $Fe_3O_4$@$SiO_2$ magnetic composite nanoparticles by a one-pot process, *Int. J. Miner. Metall. Mater.*, 23 (9), 1112–1118.

[46] Ding, H., Zhao, Y., Duan, Q., Wang, J., Zhang, K., Ding, G., Xie, X., and Ding, C., 2017, Efficient removal of phosphate from aqueous solution using novel magnetic nanocomposites with $Fe_3O_4$@$SiO_2$ core and mesoporous $CeO_2$ shell, *J. Rare Earths*, 35 (10), 984–994.

[47] Prasetya A.D., Fisli, A., Sulungbudi, G.T., Richtiara, G.C., Muslih, M.R., Mujamilah, M., Wildan, Z.L., Firda, Y., 2021, Effect of magnetic and silica ratio on the synthesis of magnetic mesoporous silica particles, *AIP Conf. Proc.*, 2381 (1), 020060.

[48] Wang, J., Shah, Z.H., Zhang, S., and Lu, R., 2014, Silica-based nanocomposites via reverse microemulsions: Classifications, preparations, and applications, *Nanoscale*, 6 (9), 4418–4437.

[49] Ab Rahman, I., and Padavettan, V., 2012, Synthesis of silica nanoparticles by sol-gel: Size-dependent properties, surface modification, and applications in silica-polymer nanocomposites—A review, *J. Nanomater.*, 2012, 132424.

[50] Ta, T.K.H., Trinh, M.T., Long, N.V., Nguyen, T.T.M., Nguyen, T.L.T., Thuoc, T.L., Phan, B.T., Mott, D., Maenosono, S., Tran-Van, H., and Le, V.H. 2016, Synthesis and surface functionalization of $Fe_3O_4$-$SiO_2$ core-shell nanoparticles with 3-glycidoxypropyltrimethoxysilane and 1,1′-carbonyldiimidazole for bio-applications, *Colloids Surf., A*, 504, 376–383.

[51] Lee, A.H.F., Gessert, S.F., Chen, Y., Sergeev, N.V., and Haghiri, B., 2018, Preparation of iron oxide silica particles for Zika viral RNA extraction, *Heliyon*, 4 (3), e00572.

[52] Dahdouh, E., Lázaro-Perona, F., Romero-Gómez, M.P., Mingorance, J., and García-Rodriguez, J., 2021, Ct values from SARS-CoV-2 diagnostic PCR assays should not be used as direct estimates of viral load, *J. Infect.*, 82 (3), 414–451.

[53] Dang, F., Enomoto, N., Hojo, J., and Enpuku, K., 2010, Sonochemical coating of magnetite nanoparticles with silica, *Ultrason. Sonochem.*, 17 (1), 193–199.